J. Phys. B: At. Mol. Opt. Phys. **31** (1998) 859–872. Printed in the UK PII: S0953-4075(98)87277-5

Electron excitation out of the $2\,^3S$ metastable level of He into high-n triplet levels

Garrett A Piech, J Ethan Chilton, L W Anderson and Chun C Lin
Department of Physics, University of Wisconsin-Madison, Madison, WI 53706, USA

Received 12 September 1997

Abstract. We report cross section results for electron excitation out of the $2\,^3S$ metastable level of He into the $5\,^3P$, $6\,^3S$, $6\,^3P$, $6\,^3D$, $7\,^3S$, $7\,^3P$, $7\,^3D$, $8\,^3S$, $8\,^3P$ and $8\,^3D$ levels for energies from onset to 18 eV. For each level, we use the optical method to measure the apparent cross section, which equals the sum of the direct excitation cross section and the cascade cross section. The direct cross section is then determined for each level by subtracting the measured cascade cross section from the apparent cross section. The shape of the excitation function is similar for levels of the same L and different n, but different for the S, P, and D families. The characteristic shapes for these three families closely resemble the corresponding ones for excitation out of the ground state of the Na atom. Trends of cross section versus principal quantum number, n, are also analysed and compared with theoretical predictions.

1. Introduction

Accurate cross sections for electron-impact excitation out of the metastable levels of rare gases are important for modelling and understanding processes that occur in gas discharge lasers, industrial plasmas and astrophysical plasmas. The magnitudes of the peak cross sections for electron excitation out of the metastable levels of He and Ar have been shown to be greater than 500–1000 times the peak magnitudes of the corresponding excitations out of the ground level (Rall *et al* 1989, Lagus *et al* 1996, Piech *et al* 1997, Boffard *et al* 1996). The behaviour of the cross sections for excitation out of the metastable levels has been found to be quite different from the behaviour of cross sections for excitation out of the ground levels. For example, it is well known that excitations out of the ground level of He corresponding to dipole-allowed transitions generally show large cross section values and excitation functions with broad maxima, whereas excitations corresponding to dipole-forbidden transitions have smaller cross sections and excitation functions with less broad maxima (Lin and Anderson 1991). Yet some excitations out of the $2\,^3S$ metastable level of He corresponding to dipole-allowed transitions have been shown to have *smaller* cross sections than excitations corresponding to dipole-forbidden transitions. Also for excitation from the He($2\,^3S$) level, the excitation functions of the dipole-allowed levels ($n\,^3P$) frequently display relatively narrow maxima, while the excitation functions of dipole-forbidden transitions ($n\,^3D$) may display relatively broad maxima (Piech *et al* 1997).

The study of electron collisions with metastable atoms is complicated by the difficulty of creating metastable atom targets of sufficient density. In the case of metastable He, experimental measurements have been made of total cross sections for electron impact on the metastable $2\,^1S$ and $2\,^3S$ levels (Wilson and Williams 1976), and ionization (Long and Geballe 1969, Dixon *et al* 1976) out of the metastable levels. More recently, measurements

0953-4075/98/040859+14$19.50

of the superelastic scattering cross sections out of the metastable levels have been made by Buckman and co-workers (Jacka *et al* 1995). In the case of electron excitation of metastable He, measurements of the differential cross sections for excitation of He($2\,^3$S) into the $n = 2$, 3 and 4 triplet levels have been made by Muller-Fiedler *et al* (1984). More recently, cross section measurements have been made of integral cross sections for excitation out of the $2\,^1$S (Lockwood *et al* 1992a) and $2\,^3$S (Rall *et al* 1989, Lockwood *et al* 1992b, Lagus *et al* 1996, Piech *et al* 1997) levels into selected higher levels. For a more complete list of the experimental work performed in electron–metastable collisions, the reader is referred to the review papers by Lin and Anderson (1991) and Trajmar and Nickel (1992). Considerable theoretical effort has also been put forward towards calculating cross sections for excitation of the metastable levels of He. A comparison of the measured cross sections with the theoretical values obtained using different methods has been presented by Lagus *et al* (1996).

To understand the systematics of excitation out of the metastable levels, a more comprehensive set of cross section data is needed. Our experiment uses a hollow cathode discharge to produce a metastable He target with a density of approximately 5×10^7 cm^{-3}; utilizing this target we can obtain signals large enough to study excitation into numerous higher levels. With this apparatus we have previously reported results for electron excitation out of the $2\,^3$S metastable level into the $n = 2$, 3, 4 and 5 triplet levels (Piech *et al* 1997). In this paper we report additional measurements of electron excitation cross sections of the $2\,^3$S metastable level into the $5\,^3$P, $6\,^3$S, $6\,^3$P, $6\,^3$D, $7\,^3$S, $7\,^3$P, $7\,^3$D, $8\,^3$S, $8\,^3$P and $8\,^3$D levels. With this larger data set, we can further analyse the trends observed for the shapes of the excitation functions and for the absolute magnitudes of the cross sections.

2. Experiment

A diagram of the experimental apparatus is shown in figure 1 and has been previously described in Piech *et al* (1997). An atomic beam of metastable He atoms is produced by a hollow cathode discharge operating at ∼7 Torr, 750 V, and 100 mA. The beam effuses out of a small (∼1 mm diameter) hole in the base of the discharge and consists of ground-state

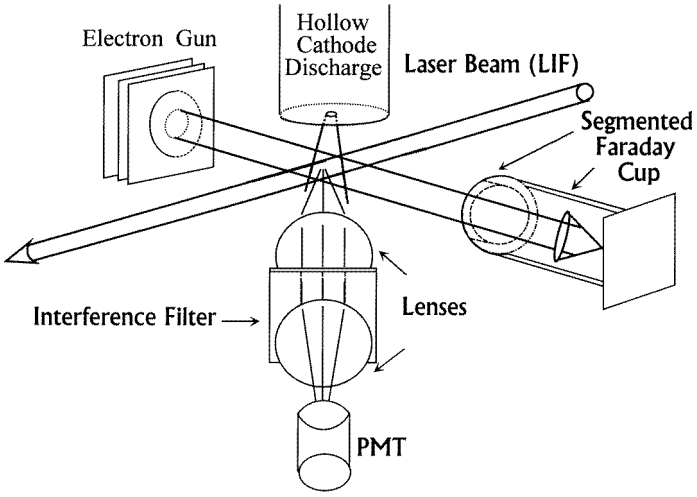

Figure 1. Diagram of experimental apparatus used.

He, $2\,^3$S metastable He, and $2\,^1$S metastable He in a ratio of approximately (3×10^7:4:1). The metastable density in the collision region is roughly 5×10^7 cm^{-3}. The atomic beam is crossed at a right angle by a low-energy electron beam produced by an electron gun with a barium oxide cathode. The electron beam excites the metastable atoms into various $n\,^3L$ higher levels. We keep the energy of the electron beam below ~20 eV so that only the metastables (rather than the ground-state atoms) in the atomic beam are excited into the various $n\,^3L$ levels. The resulting $n\,^3\mathrm{S} \rightarrow 2\,^3\mathrm{P}$, $n\,^3\mathrm{P} \rightarrow 2\,^3\mathrm{S}$ and $n\,^3\mathrm{D} \rightarrow 2\,^3\mathrm{P}$ fluorescence is collected by a system of quartz lenses, sent through a narrowband interference filter (1 nm FWHM) and imaged onto a photomultiplier tube (PMT) operating in photon-counting mode. For principal quantum numbers of $n = 6$, 7 and 8, these emissions occur in the wavelength range of 270–390 nm, thus a PMT with a quartz window (EMI 9558QA) was used. The optical axis of the detection system makes a 60° angle with the electron beam and is perpendicular to the atomic beam. The electron beam is modulated in order to subtract background counts caused by light from the hollow cathode discharge and the electron gun cathode. Counters A and B operate when the electron beam is on and off respectively, and the difference $(A - B)$ is used to determine the signal due to electron excitation only.

3. Method

The optical signal observed due to an electron collision process can generally be expressed as

$$\frac{\text{excitations observed}}{\text{volume} \times \text{sec}} = \eta \left(\frac{J}{e}\right) Qn, \tag{1}$$

where η represents the detection efficiency of the apparatus, Q the cross section for the electron excitation process, n the target density, J the current density of the electron beam, and e the charge of an electron. If η, n, and J are spatially dependent, then we more appropriately write the total signal observed as a spatial integral,

$$\frac{\text{excitations observed}}{\text{volume} \times \text{sec}} = \xi Q \int \Omega(\vec{r})[J(\vec{r})/e]n(\vec{r})\,\mathrm{d}^3\vec{r}. \tag{2}$$

Here we have broken the detection efficiency η into two parts: ξ, which is the electronic detection efficiency of the system at the observed wavelength, and $\Omega(\vec{r})$, which represents the probability of detecting a photon emitted at location $\vec{r}$.

A detailed description of the method of absolute calibration used with this apparatus is given in Piech *et al* (1997) and Lockwood *et al* (1992a, b). Here we only briefly outline the details that are relevant for the present data set. For absolute calibration we compare the signal of the $3\,^3\mathrm{P} \rightarrow 2\,^3\mathrm{S}$ fluorescence produced by our electron beam exciting the $2\,^3$S metastables into the $3\,^3$P level to the signal of the $3\,^3\mathrm{P} \rightarrow 2\,^3\mathrm{S}$ fluorescence produced by passing a laser beam through the target atoms, optically exciting the $2\,^3$S metastables into the $3\,^3$P (laser-induced fluorescence (LIF)) in the same apparatus. Since the $2\,^3\mathrm{S} \rightarrow 3\,^3\mathrm{P}$ optical absorption cross section is known, the ratio of the fluorescence signals of the electron-beam experiment to the signal of the laser-excitation experiment allows us to determine the absolute cross section for electron excitation from $2\,^3\mathrm{S} \rightarrow 3\,^3\mathrm{P}$, eliminating the unknown optical and electronic efficiencies of the detection system.

Although the He atom beam contains both the $2\,^3$S and $2\,^1$S metastables, the observed radiation from the $n\,^3L$ levels is almost entirely due to electron excitation out of the $2\,^3$S level. The emission from the spin-changing electron-excitation process, $2\,^1\mathrm{S} \rightarrow n\,^3L$, should be quite small for two reasons. First, the fraction of $2\,^1$S in the beam is significantly less than the fraction of $2\,^3$S in the beam, and second, the spin-forbidden nature of the

$2\,^1\mathrm{S} \rightarrow n\,^3L$ excitation process causes it to have smaller cross sections than the spin-allowed $2\,^3\mathrm{S} \rightarrow n\,^3L$ excitation process. We have measured the $2\,^3\mathrm{S}$:$2\,^1\mathrm{S}$ ratio in our atomic beam using laser-induced fluorescence and have determined it to be 4:1 or greater (Lockwood *et al* 1992a, b). We also have experimentally observed the contribution of the spin-changing $2\,^1\mathrm{S} \rightarrow n\,^3L$ excitation to our signal in the onsets of our excitation functions for the $n = 3$ triplet levels (Piech *et al* 1997). Even near the onset of excitation, the peak of this spin-changing contribution to the observed signal is small ($< 15\%$) compared with the spin-conserving $2\,^3\mathrm{S} \rightarrow n\,^3L$ excitation signal. As the excitation energy increases, we expect the spin-changing signal to decrease much more rapidly than the spin-conserving signal (Lin and Anderson 1991, Lockwood 1992b). Thus for all practical purposes in our measurements, the $2\,^1\mathrm{S} \rightarrow n\,^3L$ contribution to our signal may be neglected.

The absolute excitation cross sections for $n\,^3L$ levels other than the $3\,^3\mathrm{P}$ are determined by referencing the observed signal from the $n\,^3L$ level ($n\,^3L \rightarrow m\,^3K$ emission) to the $3\,^3\mathrm{P} \rightarrow 2\,^3\mathrm{S}$ emission signal. For this purpose we utilize the known ground-state electron-excitation cross sections to eliminate the need to determine our experimental optical and electronic detection efficiencies for each $n\,^3L \rightarrow m\,^3K$ transition. We first obtain a signal for excitation out of the $2\,^3\mathrm{S}$ metastable level into the $3\,^3\mathrm{P}$ level at an electron energy of 10 eV, then we obtain a signal for excitation out of the ground level ($1\,^1\mathrm{S}$) into the $3\,^3\mathrm{P}$ level at an electron energy corresponding to the peak of the ground-state excitation function. One can express the photon-counting $2\,^3\mathrm{S} \rightarrow 3\,^3\mathrm{P}$ excitation signal $(A-B)^{3\,^3\mathrm{P}}_{\mathrm{meta}}(10\ \mathrm{eV})$ that we observe in this metastable excitation experiment as

$$(A-B)^{3\,^3\mathrm{P}}_{\mathrm{meta}}(10\ \mathrm{eV}) = \xi_{3\,^3\mathrm{P}\rightarrow 2\,^3\mathrm{S}}\, Q^{3\,^3\mathrm{P}}_{\mathrm{meta}}(10\ \mathrm{eV})\, \beta_{3\,^3\mathrm{P}\rightarrow 2\,^3\mathrm{S}} \int \Omega(\vec{r})\, n_{2\,^3\mathrm{S}}(\vec{r})\, [J^{10\ \mathrm{eV}}(\vec{r})/e]\, \mathrm{d}^3\vec{r}. \tag{3}$$

Here $\xi_{3\,^3\mathrm{P}\rightarrow 2\,^3\mathrm{S}}$ is the electronic detection efficiency of our apparatus for $3\,^3\mathrm{P} \rightarrow 2\,^3\mathrm{S}$ radiation, $Q^{3\,^3\mathrm{P}}_{\mathrm{meta}}(10\ \mathrm{eV})$ is the apparent cross section for excitation out of the $2\,^3\mathrm{S}$ metastable level into the $3\,^3\mathrm{P}$ level at 10 eV and $\beta_{3\,^3\mathrm{P}\rightarrow 2\,^3\mathrm{S}}$ is the branching ratio for the $3\,^3\mathrm{P} \rightarrow 2\,^3\mathrm{S}$ transition. Inside the spatial integral, $\Omega(\vec{r})$ is the probability of detecting a photon emitted at position $\vec{r}$, $n_{2\,^3\mathrm{S}}(\vec{r})$ is the metastable target density and $J^{10\ \mathrm{eV}}(\vec{r})$ is the current density of the 10 eV electron beam. One can also write a similar expression for the signal observed for excitation out of the ground level at the peak of the ground-state excitation function, $(A-B)^{3\,^3\mathrm{P}}_{\mathrm{gs}}(\mathrm{peak})$, using the same apparatus,

$$(A-B)^{3\,^3\mathrm{P}}_{\mathrm{gs}}(\mathrm{peak}) = \xi_{3\,^3\mathrm{P}\rightarrow 2\,^3\mathrm{S}}\, Q^{3\,^3\mathrm{P}}_{\mathrm{gs}}(\mathrm{peak})\, \beta_{3\,^3\mathrm{P}\rightarrow 2\,^3\mathrm{S}} \int \Omega(\vec{r})\, n_{\mathrm{gs}}(\vec{r})\, [J^{\mathrm{peak}}(\vec{r})/e]\, \mathrm{d}^3\vec{r}. \tag{4}$$

Here $Q^{3\,^3\mathrm{P}}_{\mathrm{gs}}(\mathrm{peak})$ is the apparent cross section for electron excitation out of the ground state into the $3\,^3\mathrm{P}$ level at the peak of the excitation function, $n_{\mathrm{gs}}(\vec{r})$ is the ground-state target density, and $J^{\mathrm{peak}}(\vec{r})$ is the current density of the electron beam with an electron energy corresponding to the peak of the ground-state excitation function.

One then performs the same experiment, but now observes emission from the $n\,^3L$ level of interest,

$$(A-B)^{n\,^3L}_{\mathrm{meta}}(10\ \mathrm{eV}) = \xi_{n\,^3L\rightarrow m\,^3K}\, Q^{n\,^3L}_{\mathrm{meta}}(10\ \mathrm{eV})\, \beta_{n\,^3L\rightarrow m\,^3K} \int \Omega(\vec{r})\, n_{2\,^3\mathrm{S}}(\vec{r})\, [J^{10\ \mathrm{eV}}(\vec{r})/e]\, \mathrm{d}^3\vec{r}, \tag{5}$$

$$(A-B)^{n\,^3L}_{\mathrm{gs}}(\mathrm{peak}) = \xi_{n\,^3L\rightarrow m\,^3K}\, Q^{n\,^3L}_{\mathrm{gs}}(\mathrm{peak})\, \beta_{n\,^3L\rightarrow m\,^3K} \int \Omega(\vec{r})\, n_{\mathrm{gs}}(\vec{r})\, [J^{\mathrm{peak}}(\vec{r})/e]\, \mathrm{d}^3\vec{r}. \tag{6}$$

We can now combine equations (3)–(6) to eliminate the unknown detection efficiencies, obtaining an expression for the metastable excitation cross section into the $n\,^3L$ level in

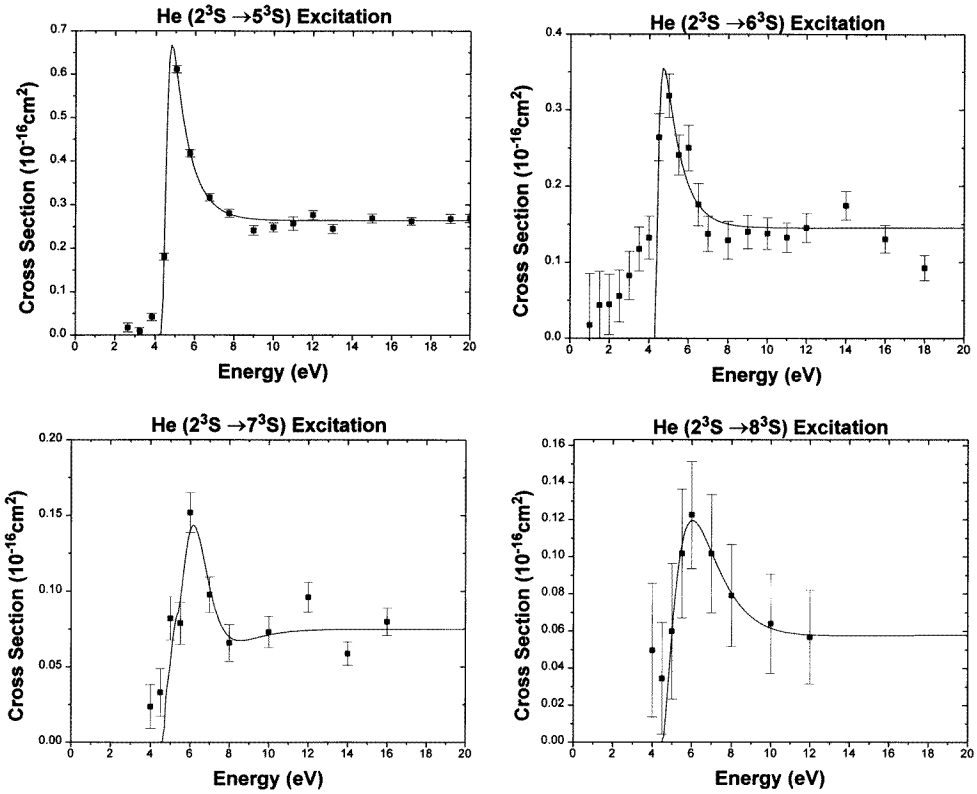

Figure 2. Apparent cross sections for He($2\,^3\mathrm{S} \rightarrow n\,^3\mathrm{S}$) excitations. Error bars shown represent statistical error only. The curve is a least-squares fit to the experimental data. See text (section 4) for comments on any nonzero data points at energies below the onset of the full curve.

terms of known or easily measurable quantities,

$$Q^{n\,^3L}_{\mathrm{meta}}(10\ \mathrm{eV}) = \left[\frac{(A-B)^{n\,^3L}_{\mathrm{meta}}(10\ \mathrm{eV})}{(A-B)^{n\,^3L}_{\mathrm{gs}}(\mathrm{peak})}\right]\left[\frac{(A-B)^{3\,^3\mathrm{P}}_{\mathrm{gs}}(\mathrm{peak})}{(A-B)^{3\,^3\mathrm{P}}_{\mathrm{meta}}(10\ \mathrm{eV})}\right] \times \left[\frac{Q^{n\,^3L}_{\mathrm{gs}}(\mathrm{peak})}{Q^{3\,^3\mathrm{P}}_{\mathrm{gs}}(\mathrm{peak})}\right] Q^{3\,^3\mathrm{P}}_{\mathrm{meta}}(10\ \mathrm{eV}). \tag{7}$$

Equation (7) illustrates that we need only perform the absolute calibration on one triplet level (in our case the $3\,^3\mathrm{P}$) in order to obtain absolute cross sections for all triplet levels. If at any time the absolute calibration of the $3\,^3\mathrm{P}$ cross section is revised, all other triplet cross sections can easily be rescaled using equation (7). We also note that the values obtained using equation (7) depend only upon the *ratio* of the ground-state peak cross sections used, and not upon their absolute magnitudes. It should be emphasized that both the metastable and ground-state cross sections used in equation (7) are *apparent* cross sections, that is, they represent the sum of direct excitation and cascade from all higher levels.

A number of experimental measurements have been made for electron excitation of the ground state ($1\,^1\mathrm{S}$) of He into higher triplet levels, including the works of St John *et al* (1964), Jobe and St John (1967), Moustafa Moussa *et al* (1969), van Raan *et al* (1971, 1974), and Showalter and Kay (1975). However, cross section measurements for

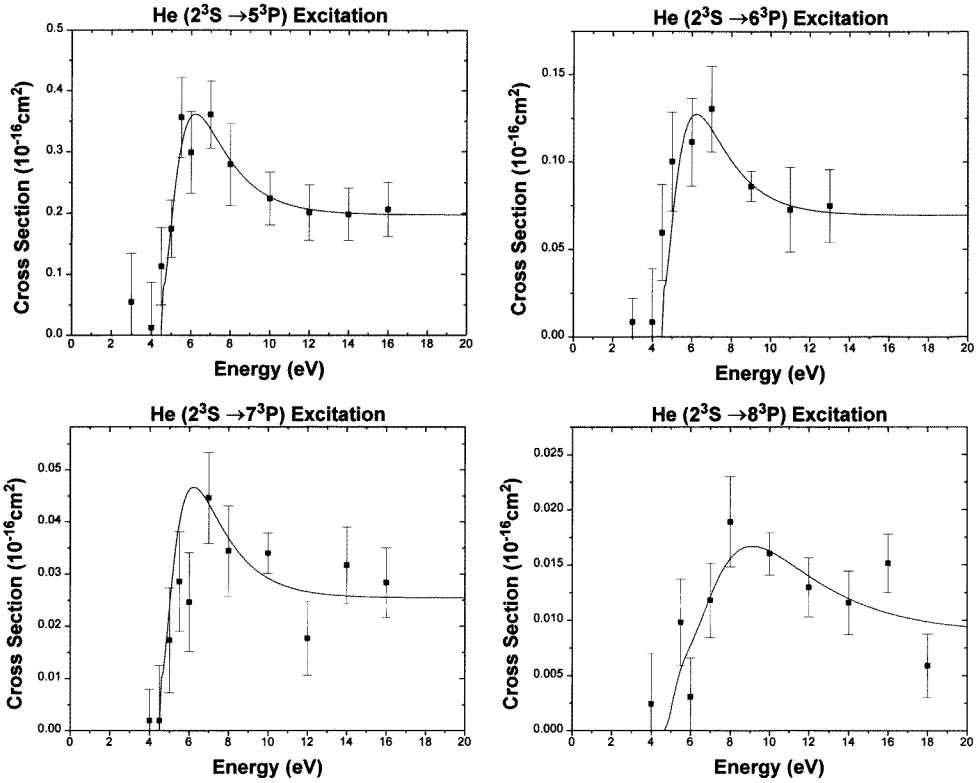

Figure 3. Apparent cross sections for He($2\,^3\mathrm{S} \rightarrow n\,^3\mathrm{P}$) excitations. Error bars shown represent statistical error only. The curve is a least-squares fit to the experimental data (see text).

excitation into levels with $n > 5$ are generally not available. An additional complication to this scarcity of data is that the apparent cross sections obtained from optical measurements often vary with pressure. Therefore we need apparent cross sections for excitation out of the ground level that are measured at the pressure at which we perform our experiment. For these reasons we decided to measure ourselves all of the $1\,^1\mathrm{S} \rightarrow n\,^3L$ peak apparent cross sections for the $n\,^3\mathrm{S}$, $n\,^3\mathrm{P}$ and $n\,^3\mathrm{D}$ levels up to $n = 8$. The apparatus we used to measure these ground-state cross sections has been previously described by Fillipelli *et al* (1984). We measured apparent cross sections and took excitation functions at pressures varying from 1 to 20 mTorr. In order to be sure that our ground-state cross sections were measured at the same pressure as is used in the metastable apparatus, we compared the shapes of the $n\,^3\mathrm{D}$ excitation functions taken by the two different apparatuses. The $n\,^3\mathrm{D}$ excitation functions will vary dramatically in shape as the pressure changes due to the large amount of pressure-dependent cascade that they receive (Lin and St John 1962). When we performed this comparison, we found that all of our measurements taken with the metastable apparatus corresponded to ground-state pressures from 7.5 to 12 mTorr. In calculating metastable cross sections from equation (7) we therefore used ground-state cross sections measured at the appropriate pressures for each set of data taken.

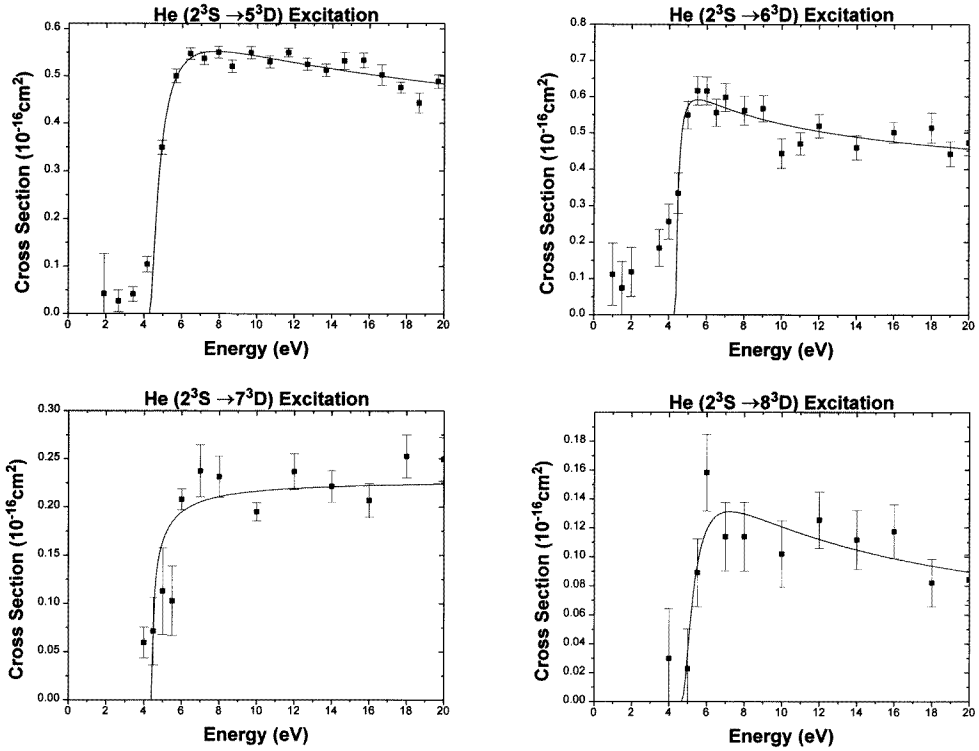

Figure 4. Apparent cross sections for He($2\,^3\mathrm{S} \rightarrow n\,^3\mathrm{D}$) excitations. Error bars shown represent statistical error only. The curve is a least-squares fit to the experimental data. See text (section 4) for comments on any nonzero data points at energies below the onset of the full curve.

4. Results

Figures 2–4 show our results for apparent excitation cross sections out of the $2\,^3\mathrm{S}$ level into the $n = 5$, 6, 7 and 8 levels. In these graphs the appearance of any nonzero data points at energies slightly below the $2\,^3\mathrm{S} \rightarrow n\,^3L$ excitation threshold (onset of the full curve) may be due to one or more of the following: (i) the uncertainty in determining the electron energy (Filippelli *et al* 1994), (ii) the energy spread ($\sim$0.6 eV) of the electron beam and (iii) excitation of the small fraction of the metastable atoms that are in the $2\,^1\mathrm{S}$ level because the $2\,^1\mathrm{S} \rightarrow n\,^3L$ excitation has a smaller energy threshold than the $2\,^3\mathrm{S} \rightarrow n\,^3L$ excitation. We obtain the numerical values of the measured apparent cross sections, shown in table 1, from the smooth curves drawn through the data shown in figures 2–4. The relatively broad ($n\,^3\mathrm{D}$) curves are obtained by a statistically weighted least-squares curve fitting routine with three free parameters based on an analytical function from Rost and Pattard (1997). The curves for the sharply peaked excitation functions ($n\,^3\mathrm{S}, n\,^3\mathrm{P}$) were obtained by fitting an exponential function with four free parameters.

We have included updated results of our previous measurements (Piech *et al* 1997) for excitation into the $5\,^3\mathrm{S}$ and $5\,^3\mathrm{D}$ levels in order to more completely illustrate the similarities for the excitation function shape within each $n\,^3L$ family. Within the uncertainties of the measurements, the shapes of the excitation functions show the same pattern as has been observed for the $n = 3$ and 4 levels (Piech *et al* 1997). The $2\,^3\mathrm{S} \rightarrow n\,^3\mathrm{S}$ excitations are

Table 1. Values obtained for $2\,^3\mathrm{S} \rightarrow n\,^3L$ apparent excitation cross sections. All values are in units of 10^{-16} cm^2. The uncertainty given for the values at 10 eV represents the uncertainty in the absolute calibration of the $3\,^3\mathrm{P}$ level using our LIF technique (±45%) plus the uncertainty in the relative calibration of each $n\,^3L$ level to the $3\,^3\mathrm{P}$ level using equation (7).

	$Q^{\mathrm{app}}(2\,^3\mathrm{S} \rightarrow n\,^3L)$										
	Incident electron energy (eV)										
Level	2	4	5	6	7	8	**10**	12	14	16	18
$2\,^3\mathrm{P}$	164.2	233.8	231.5	224.8	216.7	208.5	**193.3±96.6**	180.2	169.0	159.4	151.1
$3\,^3\mathrm{S}$	0.000	7.614	4.928	4.398	4.255	4.164	**4.003±2.00**	3.855	3.717	3.589	3.469
$3\,^3\mathrm{P}$	0.000	4.466	3.897	3.174	2.760	2.490	**2.167±0.97**	2.009	1.934	1.899	1.883
$3\,^3\mathrm{D}$	0.000	5.399	8.729	9.632	9.759	9.611	**9.082±4.54**	8.525	8.022	7.583	7.200
$4\,^3\mathrm{S}$	0.000	0.135	1.522	0.874	0.727	0.706	**0.682±0.341**	0.663	0.650	0.642	0.637
$4\,^3\mathrm{P}$	0.000	0.133	0.807	0.720	0.597	0.518	**0.436±0.218**	0.402	0.389	0.383	0.381
$4\,^3\mathrm{D}$	0.000	0.285	1.279	1.577	1.693	1.736	**1.736±0.868**	1.696	1.645	1.594	1.545
$5\,^3\mathrm{S}$	0.000	0.000	0.628	0.380	0.300	0.275	**0.265±0.132**	0.264	0.264	0.264	0.264
$5\,^3\mathrm{P}$	0.000	0.000	0.183	0.357	0.337	0.286	**0.226±0.113**	0.206	0.200	0.198	0.198
$5\,^3\mathrm{D}$	0.000	0.000	0.373	0.520	0.548	0.552	**0.542±0.271**	0.528	0.515	0.503	0.492
$6\,^3\mathrm{S}$	0.000	0.000	0.325	0.201	0.162	0.151	**0.146±0.073**	0.145	0.145	0.145	0.145
$6\,^3\mathrm{P}$	0.000	0.000	0.064	0.126	0.119	0.101	**0.080±0.040**	0.073	0.070	0.070	0.070
$6\,^3\mathrm{D}$	0.000	0.000	0.573	0.587	0.569	0.552	**0.524±0.262**	0.504	0.488	0.475	0.465
$7\,^3\mathrm{S}$	0.000	0.000	0.077	0.137	0.104	0.071	**0.071±0.036**	0.074	0.075	0.075	0.075
$7\,^3\mathrm{P}$	0.000	0.000	0.024	0.046	0.043	0.037	**0.029±0.014**	0.027	0.026	0.026	0.025
$7\,^3\mathrm{D}$	0.000	0.000	0.164	0.195	0.205	0.211	**0.216±0.108**	0.219	0.221	0.222	0.223
$8\,^3\mathrm{S}$	0.000	0.000	0.058	0.119	0.103	0.081	**0.062±0.039**	0.058	0.058	0.058	0.058
$8\,^3\mathrm{P}$	0.000	0.000	0.002	0.007	0.012	0.016	**0.016±0.014**	0.014	0.012	0.011	0.010
$8\,^3\mathrm{D}$	0.000	0.000	0.036	0.120	0.131	0.129	**0.120±0.064**	0.111	0.104	0.098	0.093

sharply peaked, the $2\,^3\mathrm{S} \rightarrow n\,^3\mathrm{P}$ excitations are less so, and the $2\,^3\mathrm{S} \rightarrow n\,^3\mathrm{D}$ excitations are broad. Numerical values of the measured apparent cross section values (obtained from the least-squares fits to the data points) are also presented in table 1. For the cross sections at 10 eV, the total error estimates (statistical and systematic) are given. For each $n\,^3L$ level, this error is made up of both the 45% absolute calibration error of the $3\,^3\mathrm{P}$ level (see Piech *et al* 1997), along with error from the relative calibration of the $n\,^3L$ level to the $3\,^3\mathrm{P}$ level using equation (7). For the $n = 3$ and 4 levels as well as the $5\,^3\mathrm{S}$ and $5\,^3\mathrm{D}$ levels, Piech *et al* (1997) used the values of $Q_{\mathrm{gs}}^{n\,^3L}(\mathrm{peak})$ reported in the literature to determine the $2\,^3\mathrm{S} \rightarrow n\,^3L$ excitation cross sections in accordance with equation (7). As explained earlier it is important that the ground-state excitation cross sections be measured at the same pressure as the experiment on excitation out of the metastable levels. Thus we measured the ground-state excitation cross sections at the appropriate pressures and used them to re-analyse the data of Piech *et al* (1997). The cross sections for the $2\,^3\mathrm{P}$, $3\,^3\mathrm{S}$, $3\,^3\mathrm{P}$, $3\,^3\mathrm{D}$, $4\,^3\mathrm{S}$, $4\,^3\mathrm{P}$, $4\,^3\mathrm{D}$, $5\,^3\mathrm{S}$ and $5\,^3\mathrm{D}$ levels resulting from this re-analysis are included in table 1. These revised cross sections agree with the earlier values of Piech *et al* (1997) within the quoted errors and are believed to be more accurate than the earlier ones.

In order to determine the direct cross sections for excitation out of the $2\,^3\mathrm{S}$ level into these higher levels, we subtract the cascade contribution from the apparent excitation cross section, i.e.

$$Q_j^{\mathrm{dir}} = Q_j^{\mathrm{app}} - \sum_{i>j} Q^{\mathrm{opt}}(i \rightarrow j) \tag{8}$$

Table 2. Values obtained for $2\,^3\mathrm{S} \rightarrow n\,^3L$ direct excitation cross sections. All values are in units of 10^{-16} cm^2. The uncertainty given for the values at 10 eV represents the uncertainty in the absolute calibration of the $3\,^3$P level using our LIF technique (±45%) plus the uncertainty in the relative calibration of each $n\,^3L$ level to the $3\,^3$P level using equation (7).

	$Q^{\mathrm{dir}}(2\,^3\mathrm{S} \rightarrow n\,^3L)$										
	Incident electron energy (eV)										
Level	2	4	5	6	7	8	**10**	12	14	16	18
$2\,^3$P	164.2	220.5	214.6	207.5	199.5	191.6	**177.1±88.55**	164.8	154.3	145.3	137.6
$3\,^3$S	0.000	7.109	4.383	3.905	3.822	3.777	**3.671±1.836**	3.548	3.422	3.299	3.182
$3\,^3$P	0.000	4.351	2.435	1.889	1.550	1.311	**1.023±0.512**	0.894	0.845	0.832	0.835
$3\,^3$D	0.000	5.271	8.129	8.965	9.124	9.022	**8.578±4.289**	8.088	7.635	7.235	6.883
$4\,^3$S	0.000	0.131	1.489	0.834	0.691	0.675	**0.656±0.328**	0.639	0.627	0.619	0.615
$4\,^3$P	0.000	0.133	0.484	0.404	0.312	0.255	**0.187±0.374**	0.160	0.150	0.148	0.149
$4\,^3$D	0.000	0.285	1.102	1.320	1.443	1.509	**1.545±0.772**	1.527	1.492	1.452	1.412
$5\,^3$S	0.000	0.000	0.623	0.370	0.291	0.267	**0.258±0.129**	0.258	0.258	0.258	0.258
$5\,^3$P	0.000	0.000	0.085	0.247	0.237	0.196	**0.142±0.071**	0.124	0.119	0.119	0.119
$5\,^3$D	0.000	0.000	0.331	0.461	0.490	0.498	**0.496±0.248**	0.488	0.479	0.471	0.463
$6\,^3$S	0.000	0.000	0.324	0.199	0.160	0.149	**0.144±0.072**	0.144	0.144	0.144	0.144
$6\,^3$P	0.000	0.000	0.040	0.076	0.074	0.064	**0.047±0.024**	0.041	0.039	0.039	0.039
$6\,^3$D	0.000	0.000	0.558	0.565	0.547	0.531	**0.506±0.253**	0.488	0.474	0.463	0.454
$7\,^3$S	0.000	0.000	0.077	0.137	0.103	0.070	**0.070±0.035**	0.073	0.074	0.074	0.074
$7\,^3$P	0.000	0.000	0.012	0.020	0.020	0.017	**0.013±0.006**	0.012	0.011	0.011	0.011
$7\,^3$D	0.000	0.000	0.158	0.185	0.196	0.201	**0.208±0.104**	0.212	0.215	0.217	0.218
$8\,^3$S	0.000	0.000	0.058	0.119	0.102	0.080	**0.061±0.038**	0.058	0.058	0.058	0.058
$8\,^3$P	0.000	0.000	0.000	0.000	0.000	0.005	**0.008±0.007**	0.006	0.004	0.003	0.003
$8\,^3$D	0.000	0.000	0.033	0.115	0.126	0.124	**0.116±0.061**	0.108	0.101	0.096	0.091

where Q_j^{app} is our measured apparent excitation cross section for level j, Q_j^{dir} is the direct excitation cross section and $Q^{\mathrm{opt}}(i \rightarrow j)$ is the optical emission cross section for $i \rightarrow j$ radiation which represents the cascade contribution to level j from a higher level i. We can obtain $Q^{\mathrm{opt}}(i \rightarrow j)$, if the apparent excitation cross section for level i is known, from the relation

$$Q^{\mathrm{opt}}(i \rightarrow j) = Q_i^{\mathrm{app}} \frac{A(i \rightarrow j)}{\sum_k A(i \rightarrow k)}, \tag{9}$$

where the A's are the transition probabilities and have been calculated by Theodosiou (1987). Thus to remove the cascade terms from Q_j^{app} as set forth in equation (8), we need the apparent cross sections for the higher levels i that can decay into level j. We use our measured apparent cross sections (the best-fit values shown in table 1) for the $n\,^3$S, $n\,^3$P and $n\,^3$D levels up to $n = 8$ to determine the cascade from these levels into the lower levels. For $n > 8$ we estimate the cross sections by the procedure proposed by Piech *et al* (1997) in which the Born approximation is used to relate the measured cross sections for the $2\,^3\mathrm{S} \rightarrow 8\,^3L$ excitation to the unknown cross section for the $2\,^3\mathrm{S} \rightarrow n\,^3L$ excitation through

$$Q^{\mathrm{exp}}(2\,^3\mathrm{S} \rightarrow n\,^3L) \approx [Q(2\,^3\mathrm{S} \rightarrow n\,^3L)/Q(2\,^3\mathrm{S} \rightarrow 8\,^3L)]_{\mathrm{Born}} Q^{\mathrm{exp}}(2\,^3\mathrm{S} \rightarrow 8\,^3L), \tag{10}$$

where the cross sections with the superscript 'exp' are the measured apparent cross sections and the cross sections inside the square brackets are the direct excitation cross sections calculated by the Born approximation. This allows us to obtain cascade contributions from the S, P and D levels for $n = 9$–15. The $n\,^3$D levels will also receive cascade contributions

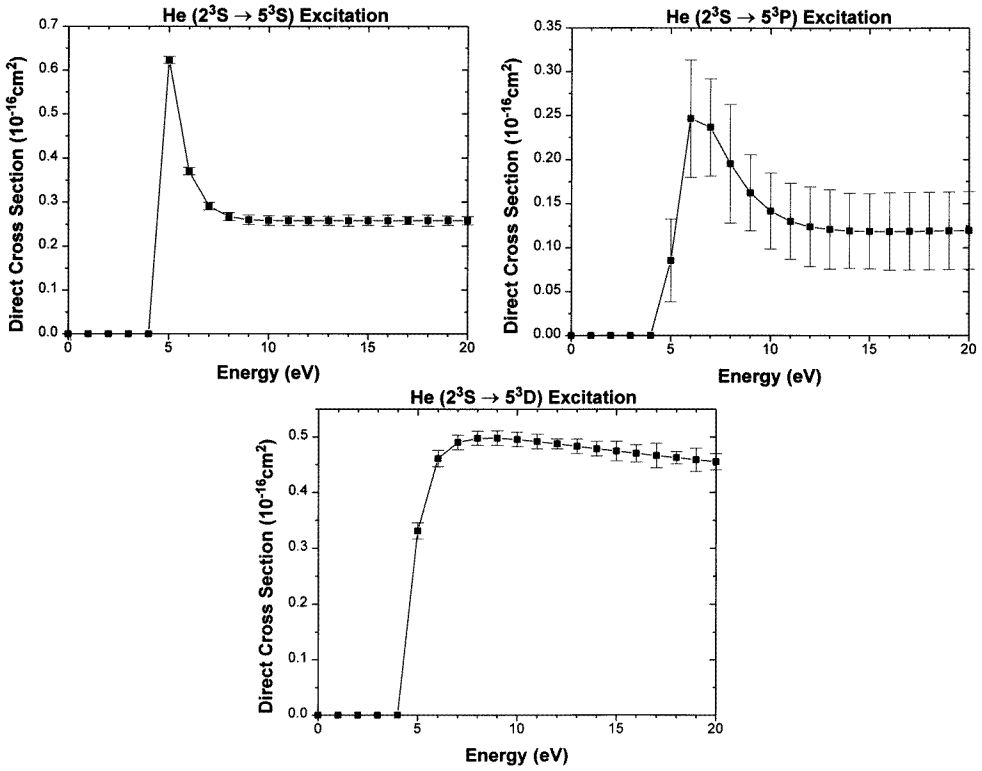

Figure 5. Direct cross sections for He($2\,^3\mathrm{S} \rightarrow 5\,^3L$) excitations calculated utilizing the least-squares fits to the apparent cross section data points (table 1 values). Error bars shown represent statistical error only.

from the $n\,^3$F levels. Since we have not measured any cross sections for the $n\,^3$F levels, we utilize the Born cross sections (direct) to estimate the cascade contribution from these levels. The cascade contributions to the $n\,^3$D levels are generally small compared with the $n\,^3$D apparent cross section (11% for the $4\,^3$D at 10 eV was the largest) on account of the very large cross sections of the $n\,^3$D family. Thus this method should introduce negligible error into our $n\,^3$D direct cross section values. Our direct cross section results are shown in table 2. As with the tabulated apparent cross section results, the cross sections at 10 eV show the total error estimates. These direct cross sections are an improvement over the results of Piech *et al* (1997) since we have measurements now for cross sections up to $n = 8$, whereas in Piech *et al* (1997) experimental measurements were available only up to $n = 5$.

The cascade contributions are typically $< 10\%$ for the $n\,^3$S levels, 35–60% for the $n\,^3$P levels (though $< 10\%$ for the $2\,^3$P due to its extremely large direct cross section) and $< 11\%$ for the $n\,^3$D levels. The general features of the excitation functions for the direct excitation cross sections are similar to those of the apparent cross sections. For illustration we show in figure 5 the excitation functions for direct excitation into the $5\,^3$S, $5\,^3$P, and $5\,^3$D levels out of the $2\,^3$S level. Again we find that the $5\,^3$S curve has the narrowest peak, the $5\,^3$D the broadest and the $5\,^3$P illustrates an intermediate behaviour. This is to be contrasted to the excitation of ground-state He in which the dipole-allowed $1\,^1\mathrm{S} \rightarrow n\,^1$P excitation functions have a much broader maximum than the dipole-forbidden $1\,^1\mathrm{S} \rightarrow n\,^1$S and the $1\,^1\mathrm{S} \rightarrow n\,^1$D

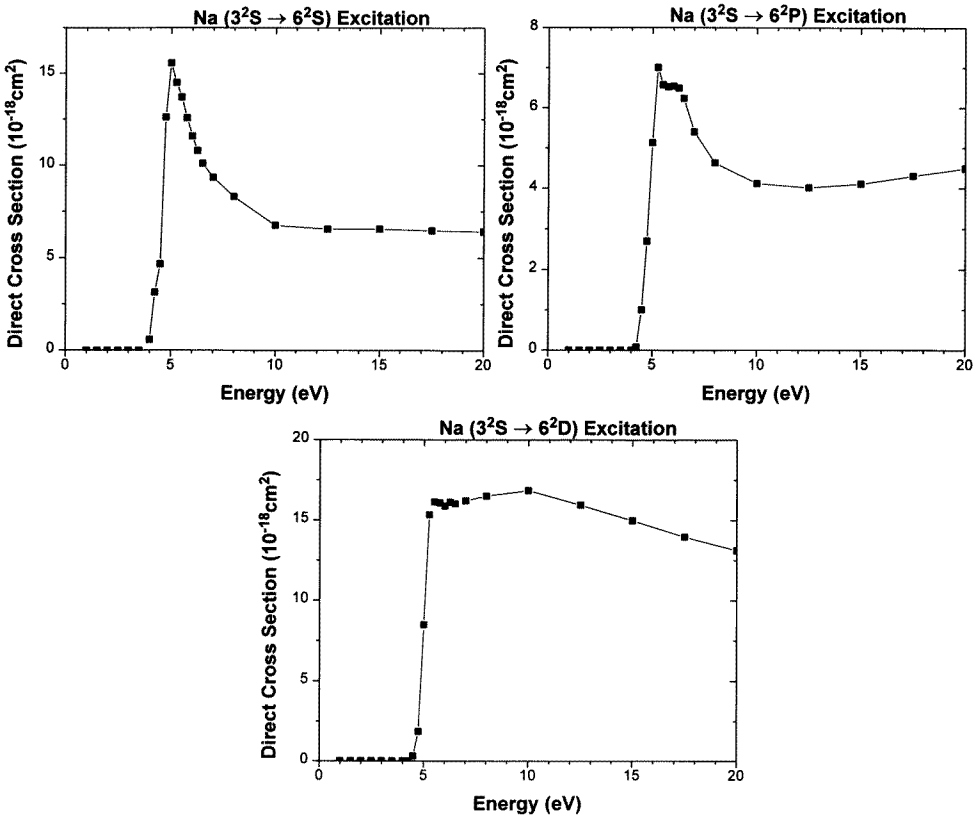

Figure 6. Direct cross sections for Na ($2\,^2\mathrm{S} \rightarrow 6\,^2L$) excitations. Data are from the paper of Phelps and Lin (1981).

excitation functions.

The presence of only one outer-shell electron in metastable He has motivated us to compare it with the alkali atoms (Piech *et al* 1997). In the case of Na, cross sections for direct excitation from the ground level into the $n\,^2$S, $n\,^2$P, and $n\,^2$D levels up to $n = 6$ have been measured (Phelps and Lin 1981). The energy dependence of the direct cross sections for the Na($3\,^2\mathrm{S} \rightarrow 6\,^2$S), Na($3\,^2\mathrm{S} \rightarrow 6\,^2$P) and Na($3\,^2\mathrm{S} \rightarrow 6\,^2$D) excitations is shown in figure 6. The three distinct shapes of the curves characteristic of the excitation into Na($n\,^2$S), Na($n\,^2$P) and Na($n\,^2$D) levels out of the Na($3\,^2$S) level are strikingly similar to those found for excitation into the He($n\,^3$S), He($n\,^3$P) and He($n\,^3$D) levels out of the He($2\,^3$S) level.

Finally we examine the variation of the excitation cross section with the principal quantum number. In figures 7–9 we plot our measured direct excitation cross sections at 10 eV for the $n\,^3$S, $n\,^3$P, and $n\,^3$D series of excitations versus n. Also included in these figures are the excitation cross sections calculated by means of the Born approximation (Chung 1997). While the Born approximation is not expected to be valid at 10 eV (which is about two to three times the threshold excitation energy) it is nevertheless useful for studying the variation of the cross sections with respect to n. In this graph the n-dependence of the measured excitation cross sections appears to match the Born results rather well. We have put the Born cross sections versus n on a log–log plot and found a fall-off somewhere

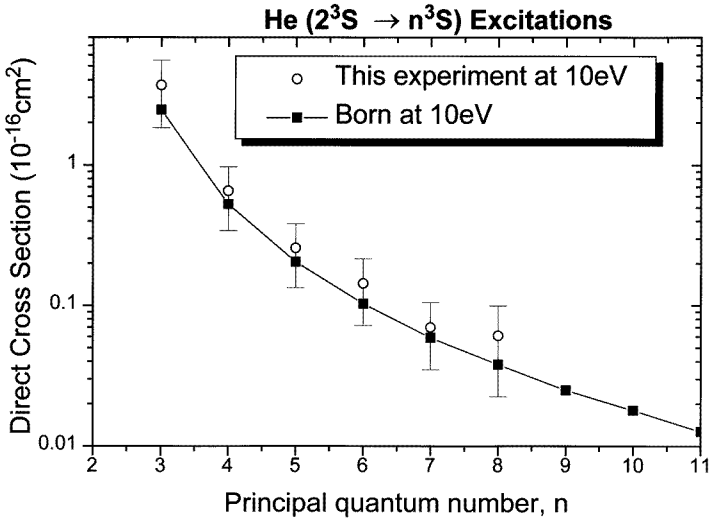

Figure 7. Direct cross section at 10 eV versus principal quantum number for He($2\,^3\mathrm{S} \rightarrow n\,^3\mathrm{S}$) excitations. The error bars shown represent the absolute experimental uncertainty for each measurement.

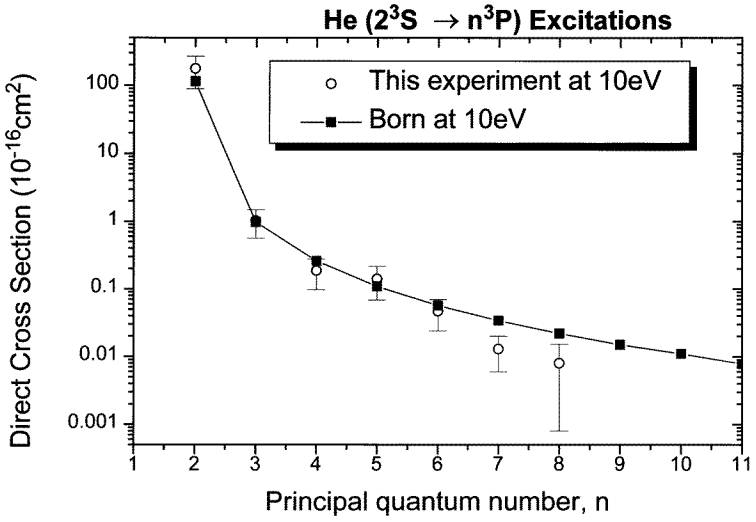

Figure 8. Direct cross section at 10 eV versus principal quantum number for He($2\,^3\mathrm{S} \rightarrow n\,^3\mathrm{P}$) excitations. The error bars shown represent the absolute experimental uncertainty for each measurement.

between n^{-3} and n^{-4}. Attempts to fit the cross sections for the $n\,^3L$ levels into the form $An^{-\alpha}$ for each L-family do not yield unequivocal results. For instance, using the Born cross sections for $n = 6$ through $n = 10$ at 10 eV for a least-square fit, we obtain $\alpha = 3.42$, 3.23 and 3.33 for the S, P and D series respectively. Repeating the curve fit for the same manifold of cross sections at 100 eV causes little change in the values of α (3.40, 3.23, 3.34) or in the quality of the fit. When we extend our fit to cover the Born cross sections for $n = 6$ through $n = 15$ at 10 eV, α becomes 3.36, 3.22 and 3.22 for the S, P and

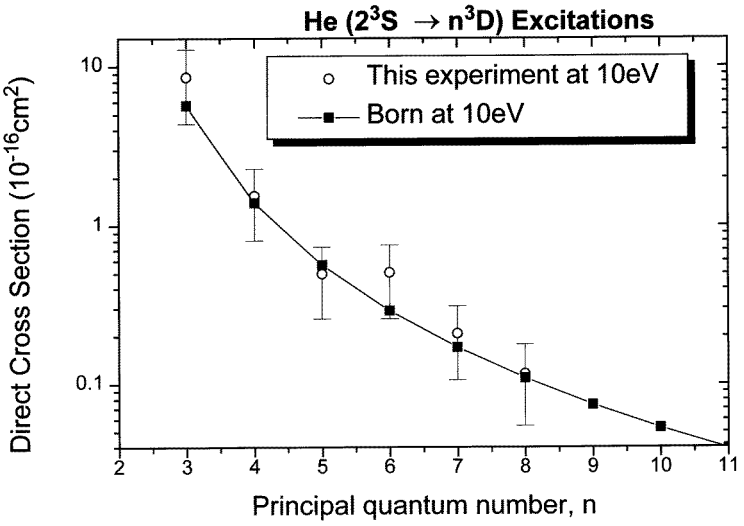

Figure 9. Direct cross section at 10 eV versus principal quantum number for He($2\,^3\mathrm{S} \rightarrow n\,^3\mathrm{D}$) excitations. The error bars shown represent the absolute experimental uncertainty for each measurement.

D levels respectively. Here we see another contrast with the (spin-conserving) excitation out of the ground level of He, $1\,^1\mathrm{S} \rightarrow n\,^1L$, for which the Born cross sections vary as $A_L n^{-3}$ for each L-family. The simple n^{-3} dependence for ground-state excitation is due to the very localized nature of the ground-state charge density so that in computing the Born integral only the portion of the excited-state wavefunction very near the origin is relevant. Thus if we represent the excited electron by hydrogenic wavefunctions, the radial function can be replaced by its first term, which varies with n as $n^{-3/2}$; hence the n^{-3} dependence in the cross sections. However, for excitation out of the $2\,^3\mathrm{S}$ level, the 2s-orbital extends over a volume corresponding to several times the Bohr radius. Consequently it is no longer sufficient to retain only the leading term of the radial nl-orbital in the Born integral, resulting in the failure of the simple n^{-3} dependence.

Acknowledgments

This work was supported by the National Science Foundation. We would like to thank Dr S Chung for providing us with his Born-approximation cross sections. We would also like to thank John B Boffard for his numerous helpful discussions.

References

Boffard J B, Piech G A, Gehrke M F, Lagus M E, Anderson L W and Lin C C 1996 *J. Phys. B: At. Mol. Opt. Phys.* **29** L795
Chung S 1997 Private communications
Dixon A J, Harrison M F A and Smith A C H 1976 *J. Phys. B: At. Mol. Phys.* **9** 2617
Filippelli A R, Chung S and Lin C C 1984 *Phys. Rev.* A **29** 1709
Filippelli A R, Lin C C, Anderson L W and McConkey J W 1994 *Adv. At. Mol. Opt. Phys.* **33** 1
Jacka M, Kelly J, Lohmann B and Buckman S J 1995 *J. Phys. B: At. Mol. Opt. Phys.* **28** L361
Jobe J D and St John R M 1967 *Phys. Rev.* **164** 117
Lagus M E, Boffard J B, Anderson L W and Lin C C 1996 *Phys. Rev.* A **53** 1505

Lin C C and Anderson L W 1991 *Adv. At. Mol. Opt. Phys.* **29** 1
Lin C C and St John R M 1962 *Phys. Rev.* **128** 1749
Lockwood R B, Anderson L W and Lin C C 1992a *Z. Phys.* D **24** 155
Lockwood R B, Sharpton F A, Anderson L W and Lin C C 1992b *Phys. Lett.* A **166** 357
Long D R and Geballe R 1969 *Phys. Rev.* A **1** 260
Moustafa Moussa H R, De Heer F J and Schutten J 1969 *Physica* **40** 517
Muller-Fiedler R, Schlemmer P, Jung K, Hotop H and Ehrhardt H 1984 *J. Phys. B: At. Mol. Phys.* **17** 259
Phelps J O and Lin C C 1981 *Phys. Rev.* A **24** 1299
Piech G A, Lagus M E, Anderson L W, Lin C C and Flannery M R 1997 *Phys. Rev.* A **55** 2842
Rall D L A, Sharpton F A, Schulman M B, Anderson L W, Lawler J E and Lin C C 1989 *Phys. Rev. Lett.* **62** 2253
Rost J M and Pattard T 1997 *Phys. Rev.* A **55** R5
Showalter J G and Kay R B 1975 *Phys. Rev.* A **11** 1899
St John R M, Miller F L and Lin C C 1964 *Phys. Rev.* **134** A888
Theodosiou C E 1987 *At. Data Nucl. Data Tables* **36** 98
Trajmar S and Nickel J C 1992 *Adv. At. Mol. Opt. Phys.* **30** 45
van Raan A F J, De Jongh J P, van Eck J and Heideman H G M 1971 *Physica* **53** 45
van Raan A F J, Moll P G and van Eck J 1974 *J. Phys. B: At. Mol. Phys.* **7** 950
Wilson W G and Williams W L 1976 *J. Phys. B: At. Mol. Opt. Phys.* **9** 423